

Supplementary material

Potential of shells of three species of eastern Australian freshwater mussels (Bivalvia: Hyriidae) as environmental proxy archives

Dilmi Herath^{A,D}, D.E. Jacob^A, Hugh Jones^B, Stewart J Fallon^C

^ADepartment of Earth and Planetary Science, Macquarie University, North Ryde, NSW 2109, Australia.

^BOffice of Environment and Heritage, PO Box A290, Sydney South, NSW 1232, Australia.

^CResearch School of Earth Sciences, Mills Road, Australian National University, Canberra, ACT 2601, Australia.

^DCorresponding author. Email: dilmi.herath@hdr.mq.edu.au

Overview of autoregressive integrated moving average (ARIMA) models

Trace element ratios were log-transformed to remove skewness and stabilise the variance. Locally-weighted polynomial regression (lowess) smoothers were superimposed on time series plots to reveal trends in trace element concentrations with shell age. This was followed by more rigorous ARIMA Time series methods to identify and describe the presence of trends, seasonality and periodicity in temporal profiles of trace element composition in two *Alathyria profuga* shells (AP04 and AP10). Model fitting was aided by an automatic model-fitting algorithm which combines unit root tests, minimisation of the AICc and MLE to obtain an ARIMA model (Khandakar and Hyndman 2008).

An autoregressive moving average model (ARMA) (p, q) process for the mean-centred $\{X_t\}$ is given as:

$$X_t - \varphi_1 X_{t-1} - \dots - \varphi_p X_{t-p} = Z_t + \theta_1 Z_{t-1} + \dots + \theta_q Z_{t-q}$$

where φ_p and θ_q are the p and q autoregressive and moving average coefficients respectively (Ariztegui *et al.* 2007). An important requirement of an ARMA(p, q) process is that the $\{X_t\}$ are stationary. Trends in the X_t series may be removed to achieve stationarity by differencing (e.g. $\nabla_1 = X_t - X_{t-1}$) to produce an integrated ARMA(p, q) or ARIMA(p, d, q) model.

ARIMA models may be modified to include seasonal parameters to represent periodic model components in a similar way to ARIMA models. Hence, we describe a multiplicative seasonal ARIMA or SARIMA model as:

$$\text{SARIMA}(p, d, q)(P, D, Q)_s$$

where the subscript s denotes the order of seasonality; e.g. $s = 12$ for a monthly time series with an annual periodicity. Refer to Brockwell and Davis (2006) or Shumway and Stoffer (2010) for further details of these models.

Regression with correlated errors (Shumway and Stoffer 2010) was used to examine the relationship of the trace element ratios Sr/Ca, Ba/Ca and Mn/Ca with temperature. The correlation structure of the residuals was identified by fitting a naïve regression model to the data, followed by fitting an ARMA model to the residuals. The regression model was then refitted with the ARMA model as the error term, by maximum likelihood estimation. The residuals were checked for white noise using the Ljung–Box white noise test and ACF plots.

Fitting of ARIMA time series model to trace element ratios

The ACF plot of the Sr/Ca time series revealed a strong seasonal cycle with a 12-month period for both shells (Fig. S7). The seasonal peaks in shell AP04 are strong for the first two seasons then dampen off before becoming indistinguishable after years 6 or 7. In shell AP10 the seasonal peaks taper off after 4–6 years.

ARIMA models were determined using the `auto.arima` function (*library forecast*) to compare a range of candidate ARIMA and SARIMA models using the AIC to select the best fitting model. The ARIMA models confirmed the presence of trend in the strontium and Barium series but not manganese. There were seasonal cycles for all trace element series in shell AP10.

Fitting of periodic regression models to $\delta^{18}\text{O}$ ratios

We fitted semi-parametric, periodic regression models (Welham *et al.* 2014) with an annual periodicity and included a nonlinear trend modelled by a penalised cubic regression smooth (Wood, 2006) to explore the pattern of trend and seasonality in the $\delta^{18}\text{O}$ series with time.

$$y_i = \beta_0 + \beta_1 \sin\left(\frac{2\pi t_i}{12}\right) + \beta_2 \cos\left(\frac{2\pi t_i}{12}\right) + s(t_i) + e_i$$

where the sine and cosine terms are dummy variables representing a seasonal cycle with a 12-month period, and $s(t_i)$ represents the cubic regression smooth of the monthly observations t_i . The β_i s are regression parameters to be estimated from the data.

Table S1. Seasonal ARIMA models selected based on the AIC criterion among candidate models

Based on the ACF and PACF plots for the time series, seasonal ARIMA models were fit to the data.

ns, not significant. $\nabla_1 = X_t - X_{t-1}$

SARIMA model	Ljung test	Mean	AR1 ϕ_1	AR2 ϕ_2	MA1 θ_1	MA2 θ_2	SAR1 Φ_1	SAR2 Φ_2	Variance
Shell AP04									
Sr (2,1,1)(2,0,0) ₁₂	ns	∇_1	0.593 (0.069)	-0.146 (0.071)	-0.980 (0.014)		0.287 (0.065)	0.292 (0.068)	0.0055
Ba (1,1,2)(2,0,0) ₁₂	ns	∇_1	0.518 (0.095)		-0.710 (0.104)	-0.257 (0.096)	0.258 (0.067)	0.316 (0.072)	0.0303
Mn (1,0,1)(2,0,0) ₁₂	ns	1.570 (0.067)	0.591 (0.066)		0.483 (0.068)		0.194 (0.067)	0.240 (0.069)	0.0271
Shell AP10									
Sr (1,0,0)(1,0,0) ₁₂	ns	1.785 (0.016)	0.591 (0.060)				0.240 (0.071)		0.0051
Ba (1,1,1)(1,0,0) ₁₂	ns	∇_1	0.662 (0.060)		-0.991 (0.024)		0.201 (0.075)		0.0401
Mn (1,0,1)	ns	1.227 (0.064)	0.604 (0.068)		0.466 (0.074)				0.0577

Table S2. Parameter estimates for regressions with correlated errors of trace element/calcium ratios (log-transformed) predicted by temperature

AR_p, autoregressive model of order p; ARMA, autoregressive moving average model. $\hat{\sigma}^2$, error variance. ns, not significant.

Trace element	Intercept	Temperature	Error model	$\hat{\sigma}^2$
Shell AP04				
Strontium	1.646 (0.064)	0.0113 (0.0034)	AR ₁ (0.54)	0.0050
Barium	-3.310 (0.104)	0.0294 (0.005)	AR ₁ (0.68)	0.0347
Manganese	1.817 (0.123)	-0.0130 (0.007) ^{ns}	AR ₂ (1.07, -0.39)	0.0296
Shell AP10				
Strontium	1.631 (0.036)	0.0084 (0.002)	AR ₁ (0.53)	0.0050
Barium	-3.124 (0.109)	0.0182 (0.006)	AR ₁ (0.61)	0.0392
Manganese	1.246 (0.160)	-0.0011 (0.008) ^{ns}	ARMA (0.60, 0.46)	0.0580

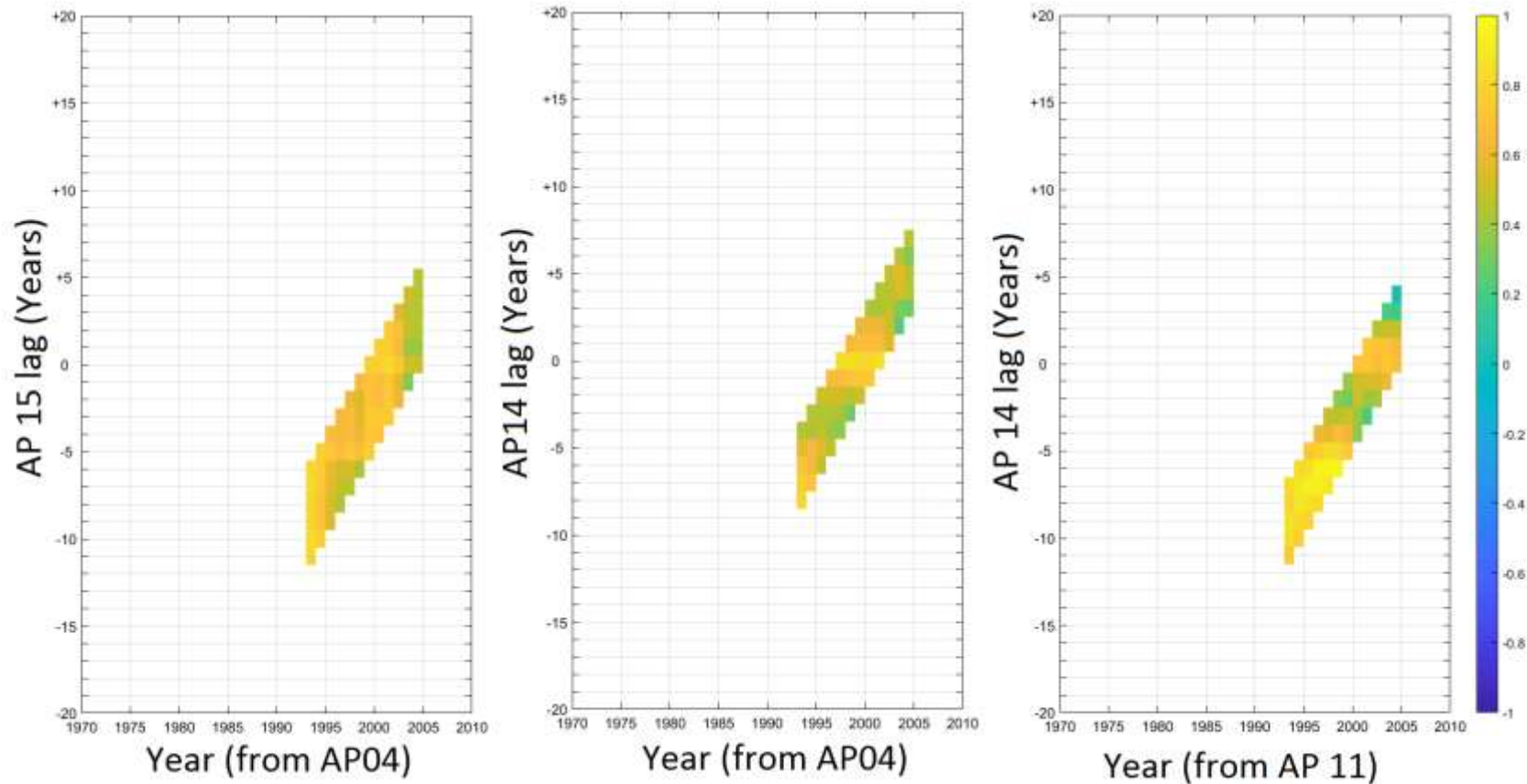


Fig. S1. Selected examples of output from the visual correlation program SHELLCORR. The images show correlation coefficients between pairs of indices width series in a sliding 21-year window at various lags. High positive correlations in yellow, high negative correlations in blue. See Scourse *et al.* (2006) for more details. Since SHELLCORR produce more than 100 images for the complete sample set, only selected examples from *Alathyria profuga* (top 6) and *Cucumerunio novaehollandiae* (bottom 3) are shown here.

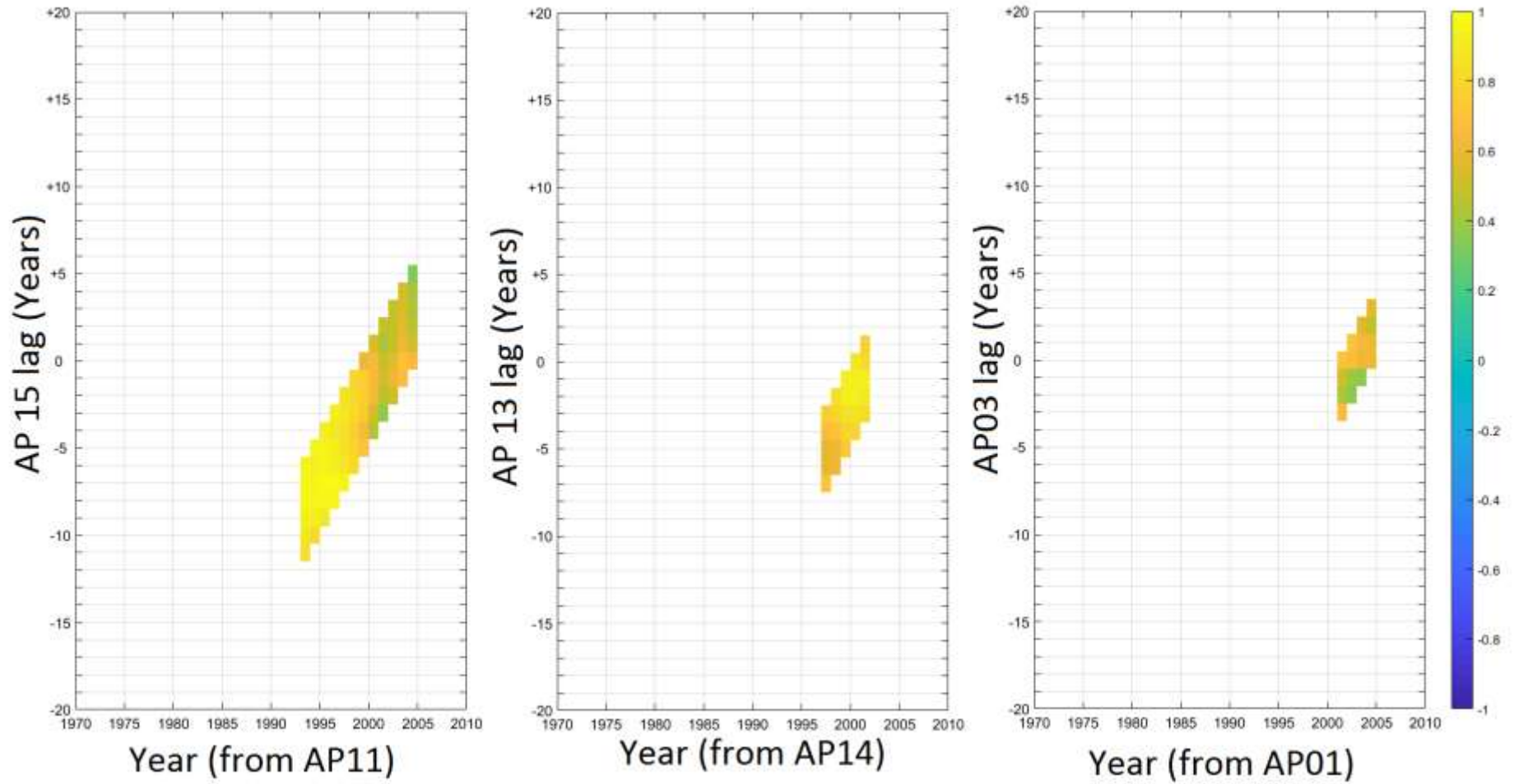


Fig. S1. (Cont.)

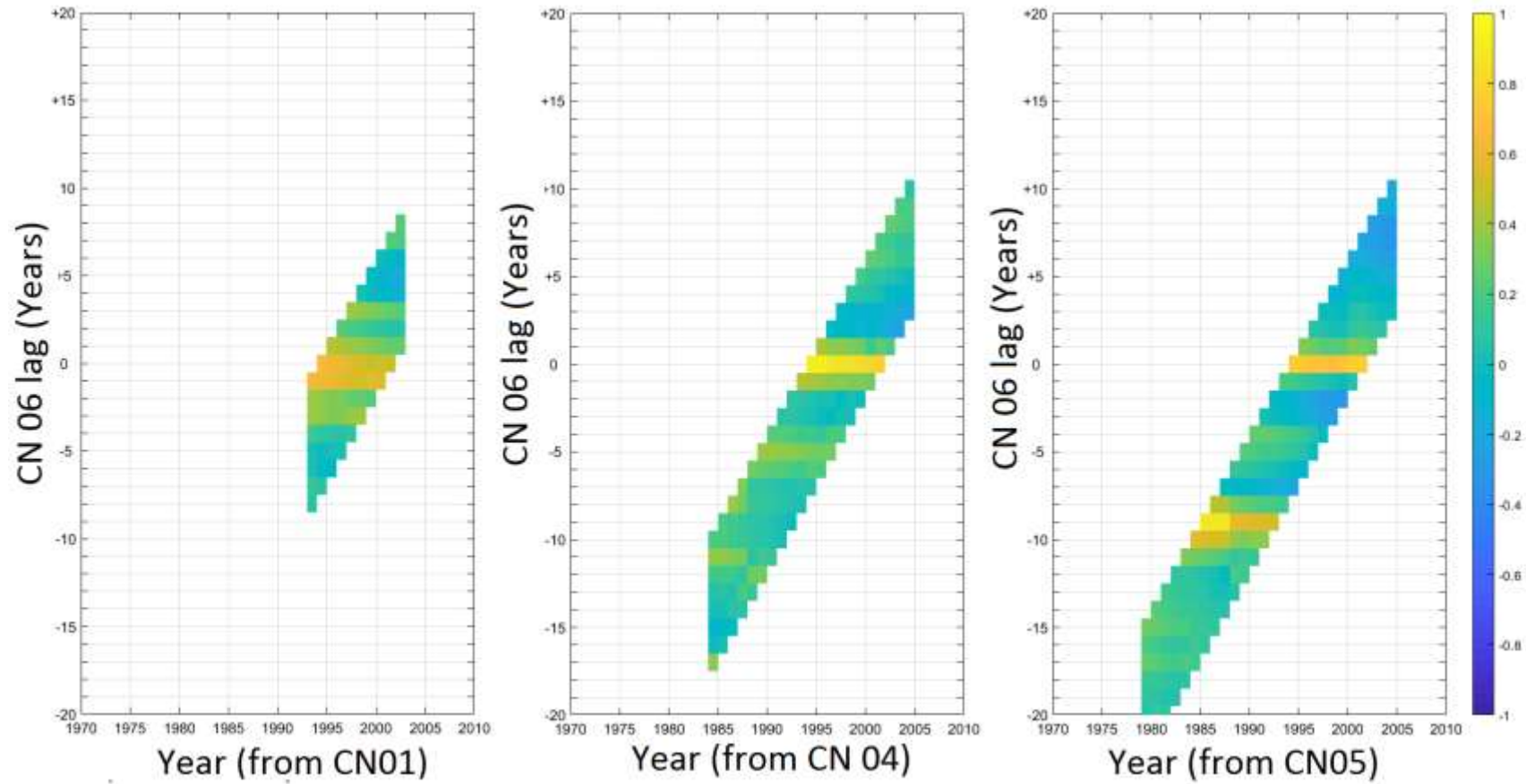


Fig. S1. (Cont.)

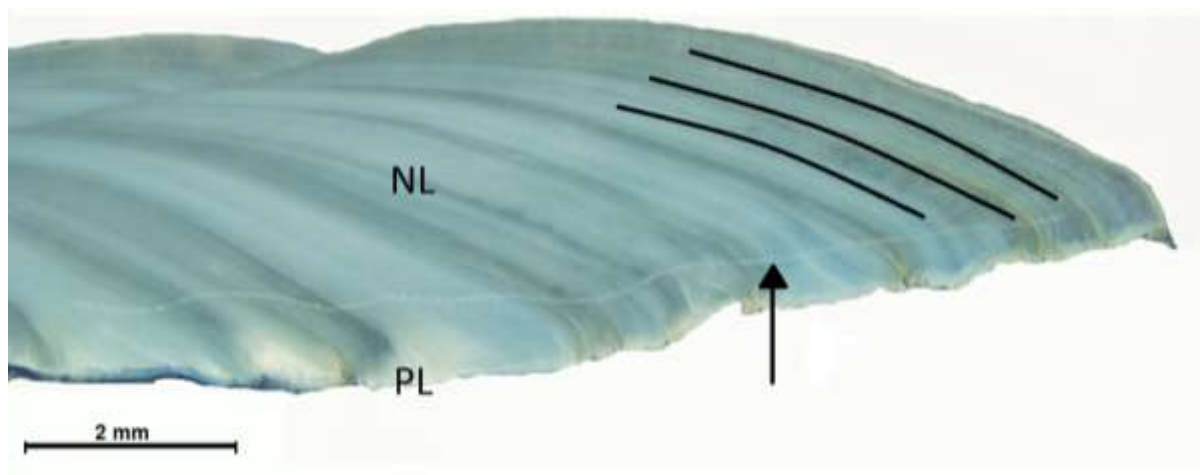


Fig. S2. Cross-sectioned, polished and stained shell of *A. profuga* to indicate where the LA-ICP-MS analysis was done (arrow). Black lines indicate example locations of the trenches drilled for oxygen isotope analysis. NL is the Nacreous layer, which is 1 to ~7 mm thick and represent >90% of the shell section. PL is the Prismatic layer, which is <1 mm thick at the bottom margin of the shell section.

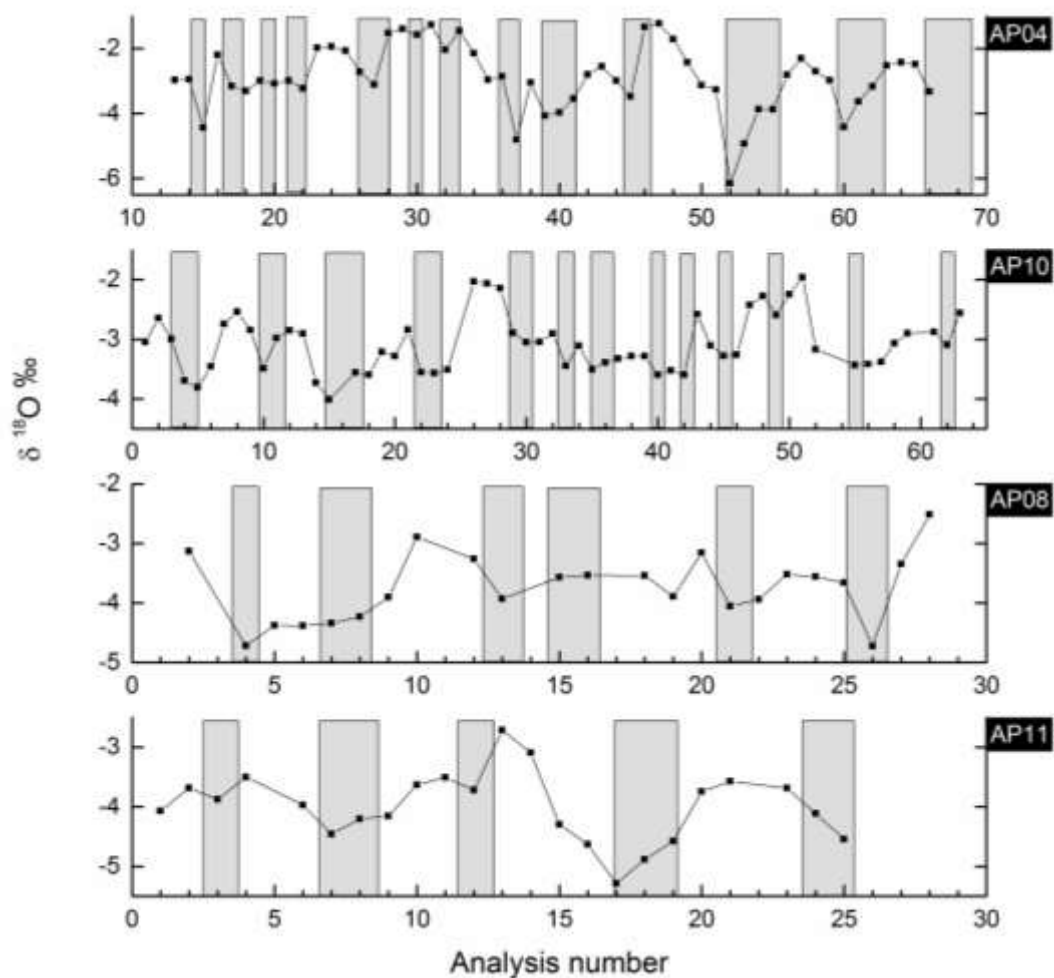


Fig. S3. $\Delta^{18}\text{O}$ (black line) variation in four *Alathyria profuga* shells indicating seasonal patterns along the direction of growth. Locations of the dark (summer) layer in the shell are indicated by the grey area. (dog, direction of growth.)

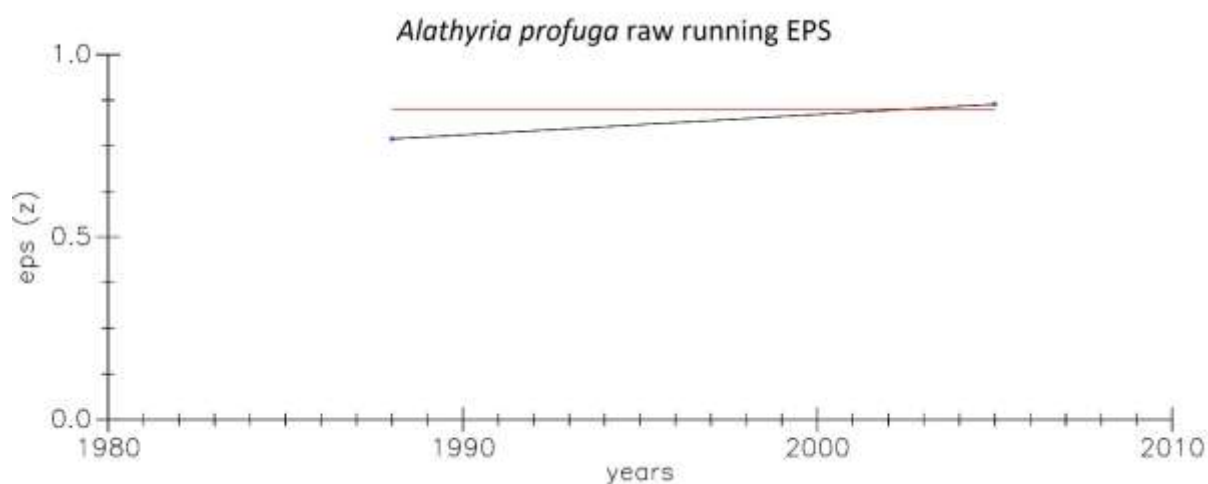


Fig. S4. Expressed population signal (EPS) for *A. profuga* calculated in a 10 year window. EPS value at the start of the window is plotted here. Red line shows the suggested threshold value of 0.85 (Wigley *et al.* 1984).

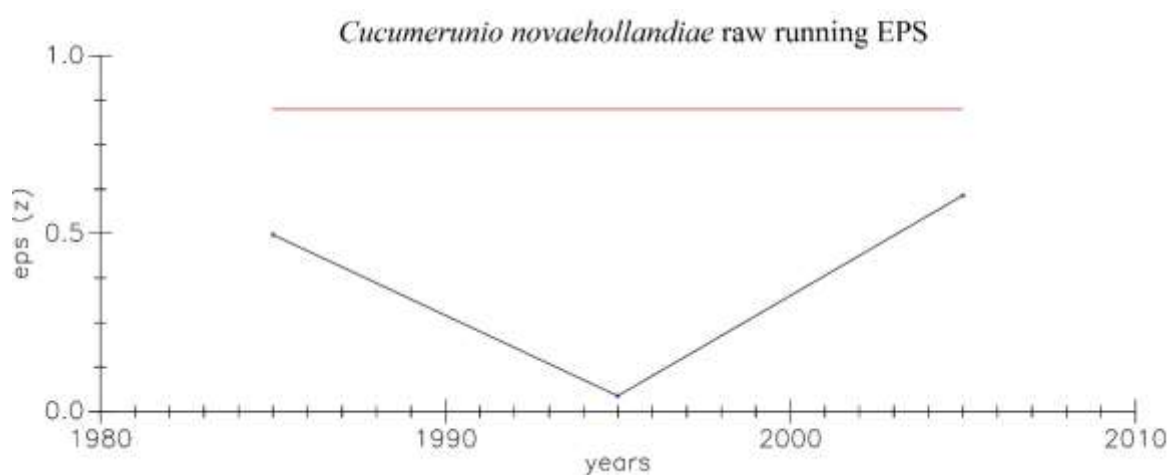


Fig. S5. Expressed population signal (EPS) for *Cucumerunio novaehollandiae* calculated in a 10-year window. EPS value at the start of the window is plotted here. Red line shows the suggested threshold value of 0.85 (Wigley *et al.* 1984).

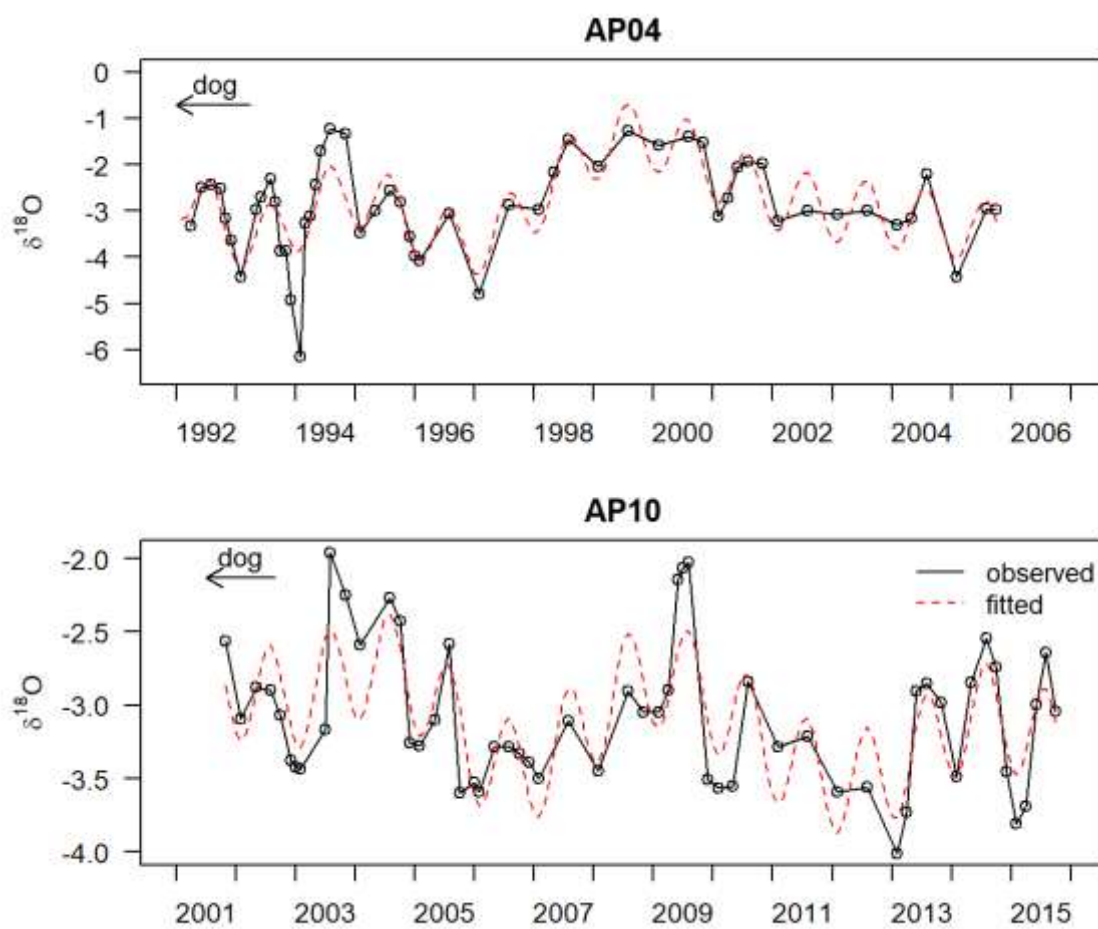


Fig. S6. Observed $\delta^{18}\text{O}$ series with fitted values from a periodic regression (with a 12-month period) from two *A. profuga* shells indicating cyclic patterns along the direction of growth. (dog, direction of growth). The period of the sinusoidal components of periodic regression closely matched the peaks and troughs in the cycles for $\delta^{18}\text{O}$.

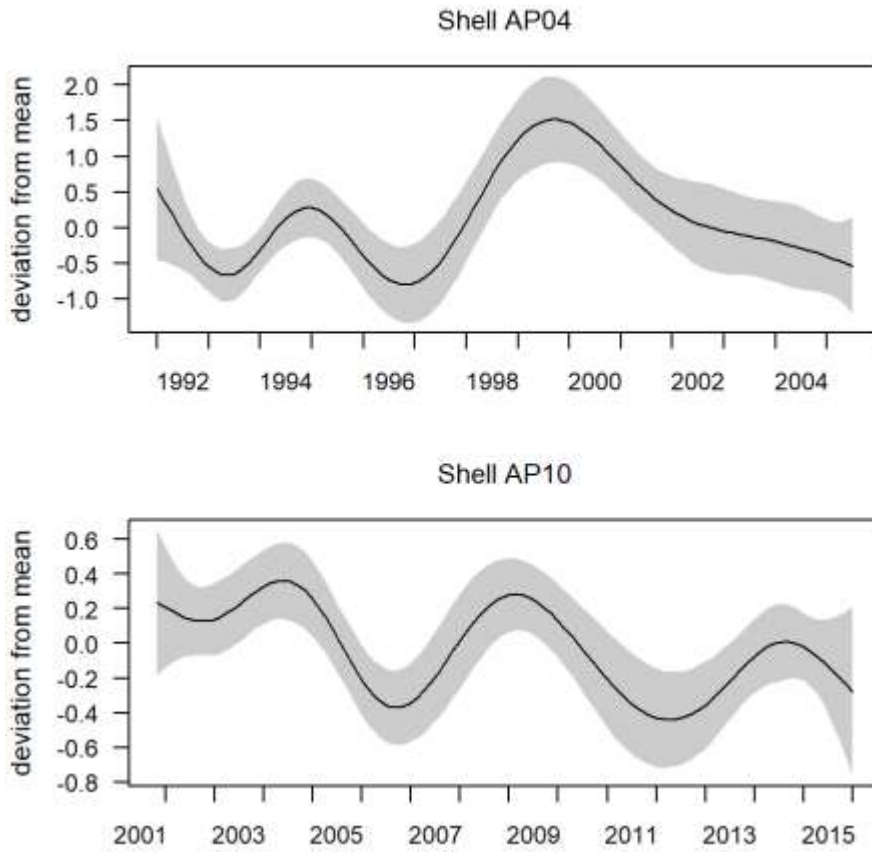


Fig. S7. Non-annual climatic seasonal cycles in $\delta^{18}\text{O}$ shell profiles.

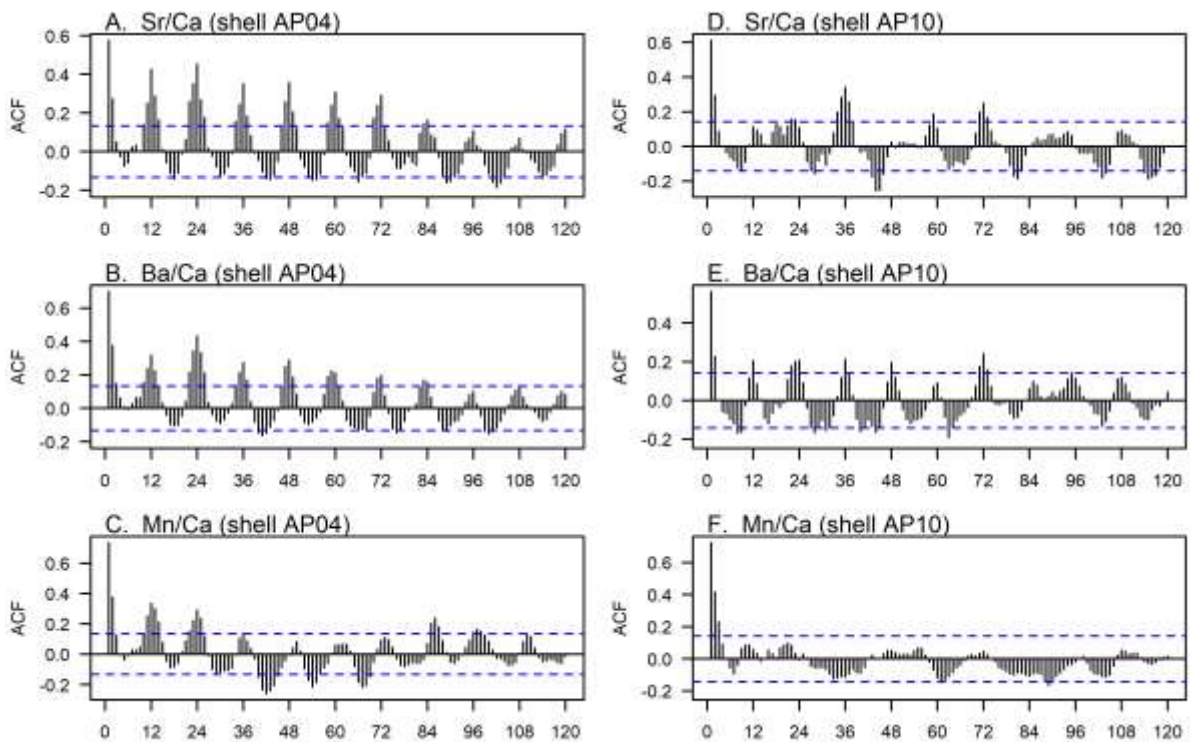


Fig. S8. Plots of the autocorrelation function for trace element ratios in shell (A,B,C) AP04 and (D,E,F) AP10.

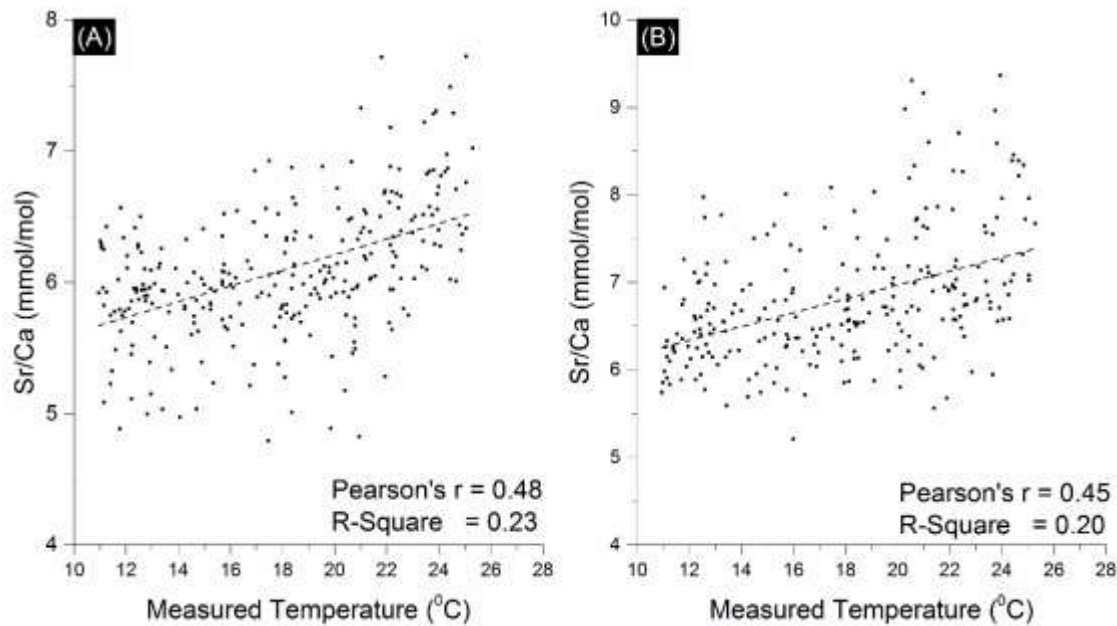


Fig. S9. Monthly averaged Sr/Ca (A) *Alathyria profuga* (n = 2) and (B) *Cucumerunio novaehollandiae* (n = 1) and measured instrumental temperatures. The dashed lines show the trend line.

References

- Ariztegui, D., Bösch, P., and Davaud, E. (2007). Dominant ENSO frequencies during the Little Ice Age in Northern Patagonia: the varved record of proglacial Lago Frias, Argentina. *Quaternary International* **161**(1), 46–55. [doi:10.1016/j.quaint.2006.10.022](https://doi.org/10.1016/j.quaint.2006.10.022)
- Brockwell, P. J., and Davis, R. A. (2006) 'Introduction to Time Series and Forecasting.' (Springer International Publishing: Basel, Switzerland.)
- Khandakar, Y., and Hyndman, R. J. (2008). Automatic time series forecasting: the forecast package for R. *Journal of Statistical Software* **27**(3), 1–22.
- Scourse, J., Richardson, C., Forsythe, G., Harris, I., Heinemeier, J., Fraser, N., Briffa, K., and Jones, P. (2006) First cross-matched floating chronology from the marine fossil record: data from growth lines of the long-lived bivalve mollusc *Arctica islandica*. *The Holocene* **16**(7), 967-974. [doi:10.1177/0959683606h1987rp](https://doi.org/10.1177/0959683606h1987rp)
- Shumway, R. H., and Stoffer, D. S. (2010) 'Time Series Analysis and its Applications: with R Examples.' (Springer Science & Business Media)
- Welham, S. J., Gezan, S. A., Clark, S., and Mead, A. (2014) 'Statistical Methods in Biology: Design and Analysis of Experiments and Regression.' (Chapman and Hall: New York, NY, USA.)
- Wigley, T. M., Briffa, K. R., and Jones, P. D. (1984). On the average value of correlated time series, with applications in dendroclimatology and hydrometeorology. *Journal of Climate and Applied Meteorology* **23**(2), 201–213. [doi:10.1175/1520-0450\(1984\)023<0201:OTAVOC>2.0.CO;2](https://doi.org/10.1175/1520-0450(1984)023<0201:OTAVOC>2.0.CO;2)
- Wood, S. (2006) 'Generalized Additive Models: an Introduction with R.' (Chapman and Hall: New York, NY, USA.)